

HIGH ANGLE-OF-ATTACK STABILITY-AND-CONTROL ANALYSIS*

Robert F. Stengel
The Analytic Sciences Corporation

SUMMARY

Methods of linear systems analysis are applied to mathematical models of aircraft flying at high angle of attack and maneuver rate. First-order longitudinal and lateral-directional coupling is obtained by linearizing the complete nonlinear equations of motion about a generalized (quasi-steady) trim point. "Open-loop" stability boundaries are defined using the linear dynamic equations, and "pilot-in-the-loop" effects are presented. Stability augmentation structures for maneuvering flight conditions are shown to be defined readily using optimal control theory.

INTRODUCTION

High-performance aircraft are susceptible to degraded flying qualities during maneuvering flight for a number of reasons. The aircraft flies at high angle of attack, α , where aerodynamic flow fields are complex and are sensitive to small variations in flight condition. Lateral-directional modes of motion are affected by the nose-high attitude, and the desirable control moments due to aileron and rudder may be overshadowed by significant adverse effects. Large roll rates may be commanded for rapid orientation of the lift vector, and the resulting gyroscopic effects couple the longitudinal and lateral-directional modes of motion. To compound the above difficulties, the pilot must adapt his control strategies to varying aircraft dynamics and control responses at high α .

Rigorous solutions to the aircraft's equations of motion are difficult to obtain in maneuvering flight. These differential equations have coefficients which are nonlinear and time varying; hence, solutions of the general equations require direct integration, either by numerical or analog computation. The resulting time histories describe the evolution of aircraft motions for given controls, disturbances, and initial conditions, and each change in any of these quantities leads to a new time history. Consequently, the nonlinear-time-varying equations are valuable for defining specific flight paths, but their complexity can obscure the identification of the underlying mechanisms which govern aircraft response.

*This work was supported by Contracts No. NAS1-13618, NASA Langley Research Center, and N00014-75-C-0432, Office of Naval Research.

This paper presents new results using linear-time-invariant dynamic equations which retain much of the coupling of the nonlinear equations but which are amenable to the comprehensive techniques of linear systems analysis. The stability characteristics of two contemporary high-performance aircraft are compared at various maneuvering flight conditions. The effects of increasing angle of attack on control response are demonstrated, and a detailed mathematical model of the human pilot is applied to the prediction of flying qualities. The fully coupled linear aircraft model also forms the basis for designing stability augmentation systems that improve handling qualities and prevent departure from controlled flight.

SYMBOLS

F	fundamental matrix of linear-time-invariant system
\underline{f}	vector of nonlinear equations of motion
G	control effect matrix of linear-time-invariant system
I	identity matrix
K	stability augmentation gain matrix
p, q, r	body-axis angular rates (roll, pitch, yaw)
t	time
\underline{u}	control variable vector
u, v, w	body-axis velocities (axial, lateral, normal)
\underline{x}	state variable vector
x_E, y_E, z_E	translational position (forward, lateral, vertical)
\underline{z}	eigenvector
α	angle of attack
β	sideslip angle
λ	eigenvalue
ϕ, θ, ψ	Euler angles (roll, pitch, yaw)
$()^T$	transpose of a vector
$(\dot{\ })$	derivative with respect to time
$\Delta()$	perturbation quantity

EQUATIONS OF MOTION

The fundamental expression of rigid-body equations of motion contains nonlinear and time-varying terms, but simplifications can be considered in certain cases. Figure 1 illustrates the classes of models which can be considered for analyzing flight motions. If the dynamic coefficients are changing rapidly with time, in comparison with the time scale of motions, the dynamic model must be time varying; if the coefficients are relatively constant, a time-invariant model will suffice. If flight motions evidence the superposition characteristic; i.e., if doubling the input doubles the output, then linear models can be used; if not, the dynamic model must be nonlinear.

The nonlinear equations of motion can be assembled in the single "state-space" (vector) equation

$$\dot{\underline{x}} = \underline{f}(\underline{x}, \underline{u}, t) \quad (1)$$

where \underline{x} is a column vector of state (or motion) variables, \underline{u} is a vector of control variables, \underline{f} is the vector of dynamic equations, and t is time. For rigid-body motion, \underline{f} and \underline{x} each have 12 elements representing the dynamic relationships and associated variables for translational and rotational kinematics and dynamics. Using conventional notation for earth-relative position, earth-body Euler angles, and body-axis rates, the state vector can be defined as

$$\underline{x}^T = \left[x_E \ y_E \ z_E \ \middle| \ \phi \ \theta \ \psi \ \middle| \ u \ v \ w \ \middle| \ p \ q \ r \right] \quad (2)$$

where $()^T$ denotes the column vector transpose, i.e., a row vector. The control vector, \underline{u} , contains at least three elements for rotational control about all axes. Further details of the nonlinear equations of motion can be found in references 1 and 2.

Nonlinear-time-invariant models are useful if amplitude-dependent effects cannot be ignored but time variations of the coefficients are negligible. Nonlinear phenomena, such as limit cycles, subharmonic response, jump resonance, and nonlinear cross coupling may be responsible for such aircraft behavior as wing rock, porpoising (or bucking), jump response of roll rate to aileron input, and forcing of longitudinal modes by lateral oscillations during symmetric, wings-level flight (refs. 3 and 4).

The stability and control of small variations about the reference flight path can be investigated using linear dynamic models whose coefficients may vary in time as the flight condition varies. Linear-time-varying models could be required to assess aircraft stability during rapid acceleration, deceleration, or

for steep, high-speed flight paths, in which changing air density affects system dynamics (refs. 5 to 7). Reference 2 indicates that the accelerations associated with air combat maneuvering introduce time-varying coefficients in linear models; however, explicit time-varying dynamic effects were not found to be significant, and all major conclusions regarding the flight stability of the subject aircraft could be drawn from the equivalent time-invariant model.

The aircraft equations of motion can be expressed in linear form by performing a Taylor series expansion of equation (1) and retaining only first-order terms. The expansion results in

$$\dot{\underline{x}}_0 + \Delta \dot{\underline{x}} = \underline{f}(\underline{x}_0, \underline{u}_0, t) + \underline{f}_{\underline{x}} \Delta \underline{x} + \underline{f}_{\underline{u}} \Delta \underline{u} \quad (3)$$

where $\underline{f}_{\underline{x}}$ and $\underline{f}_{\underline{u}}$ are partial derivative matrices with respect to the state and control, respectively, evaluated along the nominal flight path. The nominal flight path satisfies equation (1), and the dynamics of small perturbations from the flight path are described by

$$\Delta \dot{\underline{x}} = F \Delta \underline{x} + G \Delta \underline{u} \quad (4)$$

where $\underline{f}_{\underline{x}}$ and $\underline{f}_{\underline{u}}$ are denoted by F and G and may contain time-varying coefficients.

Linear-time-invariant models describe small-perturbation stability in the vicinity of a single flight condition, and can be useful for practical approximation of system dynamics, for sensitivity analyses, and for control system design. (References 8 to 11 use linear models in the examination of dynamic coupling phenomena.) As shown in figure 1, coefficients of the linear model are defined by the local slopes at a given flight condition, and the principle of superposition applies in characterizing flight motions.

The importance of linearizing about a generalized trim condition is illustrated by figure 2, which presents linear and nonlinear responses to a large rudder input. The nonlinear model's trace demonstrates significant longitudinal/lateral-directional coupling as well as large responses in sideslip, β , and roll rate, p . The model which is linearized about the initial "wings-level" flight condition does not possess this coupling, and the magnitudes of β - p oscillations are underestimated (fig. 2a). Using the generalized trim procedure* to define a linearization

*This trim procedure, described in reference 1, numerically defines mean values of translational and rotational rates which minimize translational and rotational accelerations for given Euler angles and control settings.

point 4 sec into the maneuver introduces the missing longitudinal/lateral-directional coupling, leading to substantially improved modeling of the nonlinear system's oscillations (fig. 2b). The coupled linear system's response eventually diverges from the nonlinear response, but the fact that it stays in the proper neighborhood for several seconds suggests the utility of the linear-time-invariant model in defining local stability, in providing a baseline for control system design, and in analyzing piloting effects.

MANEUVERING EFFECTS ON STABILITY

Configuration-dependent effects and common attributes of maneuvering flight can be seen in comparisons of the stability boundaries of two contemporary high-performance aircraft. Aircraft A is a small, supersonic air superiority fighter (ref. 1); aircraft B is a larger supersonic fighter with similar mission (ref. 2).

The stability boundaries of the aircraft are defined by the conditions at which the real parts of the eigenvalues (or roots) of the linear-time-invariant dynamic equation (eq. (4)) change sign. The 12 eigenvalues, λ_i ($i=1$ to 12), of the equation are complex numbers, each of which satisfies the following equation:

$$\det(\lambda_i I - F) = 0 ; \quad i=1 \text{ to } 12 \quad (5)$$

where I is the identity matrix. Each oscillatory mode is represented by two complex-conjugate λ_i , while each convergent (or divergent) mode is represented by one real λ_i . The λ_i describe the time scales and stability of the normal modes of motion, which usually partition into a longitudinal set (short period oscillation, phugoid oscillation, and pure integrations ($\lambda_i=0$) for range and altitude) and a lateral-directional set (Dutch roll oscillation, roll and spiral convergences, and pure integrations for crossrange and yaw angle) during "wings-level" flight.

The corresponding complex-valued eigenvectors, \underline{z}_i , indicate the involvement of each motion variable in each mode, satisfying the equation

$$(\lambda_i I - F) \underline{z}_i = 0 ; \quad i=1 \text{ to } 12 \quad (6)$$

For example, in symmetric flight the two complex-conjugate eigenvectors associated with the short period oscillation normally involve large pitch rate and normal velocity components (Δq and w), small pitch angle and axial velocity components ($\Delta \theta$ and Δu), and none of the remaining longitudinal and lateral-directional

components. Thus, the \underline{z}_i are said to characterize the "shape" of each mode, while the λ_i characterize the growth or decay of the magnitude of \underline{z}_i .

Several effects of maneuvering flight can be noted. Increasing mean angle of attack or pitch rate alters the time scale, stability, and shape of each mode, but it does not couple the longitudinal and lateral-directional sets, as symmetry is maintained; therefore, the number of non-zero elements in each \underline{z}_i is unchanged. Introducing mean sideslip, roll rate, or yaw rate leads to full coupling, and it alters aircraft stability; hence, the number of non-zero elements in each \underline{z}_i increases. It is often found that symmetric variations have greatest effect on stability (due to changes in aerodynamic flow fields), while asymmetric variations have greatest effect on mode shape (as a consequence of inertial coupling).

Figure 3 illustrates the effects of α_0 and β_0 on the open-loop stability boundaries of the two aircraft at an altitude of 6100 m. The different true airspeeds, V_0 , used in analysis have small effect on the stability boundaries, although the differing dynamic pressures affect the natural frequencies and time constants of the normal modes. Aircraft A evidences an unstable phugoid mode at low α_0 and an unstable Dutch roll mode (due to negative damping) at high α_0 (fig. 3a). These results are apparently insensitive to small sideslip angles; however, there is substantial change in mode shape (not shown). Although conventional names are used, the "phugoid" mode contributes to significant roll angle motion, and the "Dutch roll" mode contains non-trivial normal velocity response. At higher sideslip angles, there are coupled, unstable oscillations and divergences, which also are found in the response of Aircraft B (fig. 3b). The latter aircraft is seen to possess unstable Dutch roll and roll-spiral oscillation bands in the vicinities of 20- and 30-deg angle of attack. Both instabilities can be traced to loss of directional restoring moments.

Fighter aircraft are capable of high roll rate, and air combat maneuvers often include such motions. For the aircraft to roll with constant aerodynamic angles, the roll rate, p_{w_0} , must occur about the wind x-axis (which is the same as the stability x-axis for constant nominal aerodynamic angles). Sideslip variations also are considered, since piloting error could easily result in non-zero β_0 during a rolling maneuver. Both positive and negative p_{w_0} are considered, to account for roll "into" or "out of" the sideslip. (The senses are opposite in the first case, identical in the second.)

The stability boundaries that result from combined roll rate and sideslip are shown in figure 4, and it is interesting to note striking similarities between the boundaries of the two aircraft. These boundaries are antisymmetric about the origin (as indicated

in fig. 4b) because positive sideslip-positive roll rate has the same effect on aircraft stability as negative sideslip-negative roll rate. Both aircraft have stable bands near $\beta_0 = 10$ deg when p_{w_0} is large, a beneficial effect of coupling. Instability is substantial when each aircraft is sideslipped "into" the roll. The eigenvectors (not shown) indicate that high p_{w_0} causes the Δp component of the short-period mode to be greater than the Δq component.

References 1 and 2 present results regarding the stability of symmetric pullups and a maneuver known as a "rolling reversal" (high-g pullup, roll, inverted flight, roll-out, and pullup). Both aircraft have lateral-directional instabilities as a result of large positive pitch rate. Aircraft A possesses an unstable Dutch roll mode during most of the 22-sec maneuver. Aircraft B evidences an unstable spiral mode for much of the maneuver, with a Dutch roll instability during the final pullup. These results predict increased pilot workload during maneuvering flight as a consequence of factors not normally considered in stability and control analyses.

CONTROL RESPONSE

Control input time histories demonstrate the transient response of Aircraft B with increasing α_0 . The lateral control input is applied for two seconds and then removed, and all responses are computed using the linear-time-invariant model. Figure 5 shows the lateral-directional responses which result. As angle of attack increases, both the system eigenvalues and the control effectiveness vary. The unstable Dutch roll mode is excited at α_0 of 20 deg, and the yaw rate response is reversed. Although the aircraft is again stable at 25 deg, the control response is poor due to the large adverse yaw response. At 30 deg, the lateral control input excites the unstable roll-spiral oscillation, which dominates the response.

Additional results contained in reference 2 indicate that longitudinal response to lateral control is about 50 percent of directional response levels when α_0 and β_0 are each 10 deg. When $p_{w_0} = 75$ deg/sec, the resulting Δq is one-third as large as Δr , and $\Delta \alpha$ response is three times greater than $\Delta \beta$ response.

PILOTING EFFECTS

The effects which the pilot has on aircraft stability can be modelled by a closed-loop system which feeds back aircraft motions to available control surfaces. An optimal control pilot model has been used for this purpose in references 2 and 12, and

it contains the following elements: an estimator, which processes the pilot's observations to provide an estimate of the aircraft state; a controller, which mechanizes the pilot's regulating functions and transmits the results to the neuromuscular dynamics; and a neuromuscular model, which represents the dynamics of the pilot's limbs.

Investigations of pilot-aircraft instability using the control-theoretic pilot model fall into two categories: those in which the pilot fails to stabilize an unstable aircraft, and those in which the pilot destabilizes a stable aircraft. In the first case, the pilot's time delay, observation noise, neuromuscular time constants, and scanning factors are important parameters. Assuming that the aircraft's linearized dynamics have one or more unstable eigenvalues, the analysis determines pilot parameters for which the optimal control model fails to exist. The second category is related to the pilot's ability to adapt to changing flight conditions. Pilot-induced oscillations (PIO) and departures can occur because a control strategy which is appropriate to one flight condition is destabilizing in another.

The control-theoretic pilot model can be used to analyze nonadapting pilot behavior in a straightforward manner. In the example considered here, the pilot model's control strategy is first determined at a low- α_0 flight condition. This strategy is frozen, and the aircraft's dynamics are allowed to change. The stability of the pilot-aircraft system is determined by its eigenvalues.

Nonadapted piloting effects on pilot-aircraft stability regions can be presented in the aircraft's α_0 - β_0 plane. Figure 6 shows the stability regions under the assumption that the pilot is adapted to $\alpha_0 = 10$ deg and $\beta_0 = 0$ deg. The instabilities of the longitudinal modes (phugoid and short period) are the same in both cases, since the available control is the same in both cases. Figure 6 suggests that if the pilot model does not adapt, at some point low- α_0 piloting procedure combined with adverse yaw will cause an instability. In figure 6a this occurs at $\alpha_0 \approx 17$ deg, and the incorrect procedure is characterized by an unstable (closed-loop) spiral mode. When three controls are used, the instability due to incorrect procedure does not occur until $\alpha_0 \approx 26$ deg, as shown in figure 6b. These results are compatible with experimental results obtained from manned simulation and flight test of Aircraft B.

STABILITY AUGMENTATION FOR DEPARTURE PREVENTION

Flying qualities can be improved by using an automatic system to compensate for variations in aircraft dynamic characteristics. Control logic for a Departure-Prevention Stability Augmentation System (DPSAS) can be developed using optimal control theory (refs. 1 and 2). The linear-optimal regulator is a feedback control law of the form

$$\Delta \underline{u} = -K \Delta \underline{x} \quad (7)$$

where K is a gain matrix which scales feedback and crossfeed terms for proper stabilization and compensation of the aircraft's motion (ref. 13). K varies to maintain good flying qualities for large variations in maneuvering conditions, guaranteeing closed-loop stability and accounting for all significant longitudinal/lateral-directional coupling.

Comparisons of DPSAS closed-loop response with open-loop response of the subject aircraft are presented in figures 7 and 8. Each aircraft is performing a constant-roll-rate maneuver and is subjected to a $\Delta\beta$ initial condition of 1 deg. The roll rate leads to substantial longitudinal response for both aircraft, with Aircraft A exhibiting a lightly damped oscillation in the unaugmented condition and Aircraft B possessing a real divergence. In both cases, the DPSAS quickly damps all perturbations, using gains which are specific to the aircraft and flight condition. Linear-time-invariant dynamic models can be used to develop the necessary values of K throughout the flight envelope, and gains can be scheduled in the flight control system to minimize the probability of departure.

CONCLUSION

The analysis of aircraft flying at high angle of attack and maneuver rate can be aided by considering fully coupled linear-time-invariant dynamic models. The coupled linear equations are no more difficult to handle than uncoupled longitudinal and lateral-directional sets when "state-space" methods are used, yet they capture significant aspects of maneuvering flight which otherwise would require the solution of nonlinear equations of motion. New insights regarding open-loop stability boundaries, handling qualities, and closed-loop control can be gained by direct extension of well-established methods of linear systems analysis.

REFERENCES

1. Stengel, R.F. and Berry, P.W., "Stability and Control of Maneuvering High-Performance Aircraft," TASC TR-587-1 (to appear as a NASA Contractor Report).
2. Stengel, R.F., Taylor, J.H., Broussard, J.R., and Berry, P.W., "High Angle-of-Attack Stability and Control," TASC TR-612-1 (to appear as an ONR Contractor Report).
3. Ross, A.J., "Investigation of Nonlinear Motion Experienced on a Slender-Wing Research Aircraft," J. Aircraft, Vol. 9, No. 9, Sept 1972, pp. 625-631.
4. Schoenstadt, A.L., "Nonlinear Relay Model for Post-Stall Oscillations," J. Aircraft, Vol. 12, No. 7, July 1975, pp. 572-577.
5. Haddad, E.K., "Study of Stability of Large Maneuvers of Airplanes," NASA TN D-2447, Aug 1974.
6. Curtiss, H.C., Jr., "Dynamic Stability of V/STOL Aircraft at Low Speeds," J. Aircraft, Vol. 7, No. 1, Jan-Feb 1970, pp. 72-78.
7. Ramnath, R.V. and Sinha, P., "Dynamics of the Space Shuttle During Entry into Earth's Atmosphere," AIAA Journal, Vol. 13, No. 3, Mar 1975, pp. 337-342.
8. Phillips, W.H., "Effect of Steady Rolling on Longitudinal and Directional Stability," NACA TN-1627, June 1948.
9. Abzug, M.J., "Effects of Certain Steady Motions on Small Disturbance Airplane Dynamics," J. Aeronautical Sciences, Vol. 21, No. 11, Nov 1954, pp. 749-762.
10. Stengel, R.F., "Effect of Combined Roll Rate and Sideslip Angle on Aircraft Flight Stability," J. Aircraft, Vol. 12, No. 8, Aug 1975, pp. 683-685.
11. Johnston, D.E. and Hogge, J.R., "Nonsymmetric Flight Influence on High-Angle-of-Attack Handling and Departure," J. Aircraft, Vol. 13, No. 2, Feb 1976, pp. 111-118.
12. Broussard, J.R. and Stengel, R.F., "Stability of the Pilot-Aircraft System in Maneuvering Flight," Proceedings of the 12th Annual Conference on Manual Control, May 1976.
13. Kwakernaak, H. and Sivan, R., Linear Optimal Control Systems, Wiley-Interscience, New York, 1972.

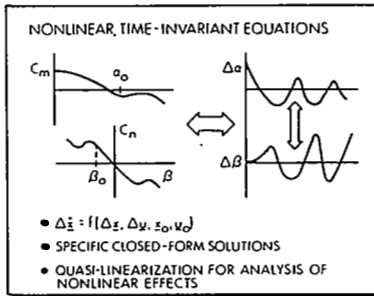
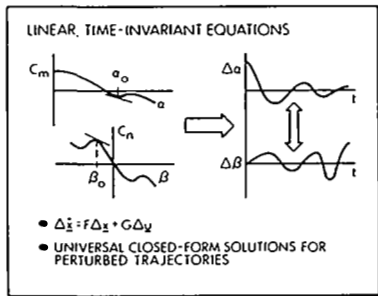
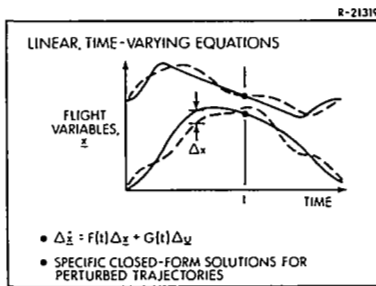
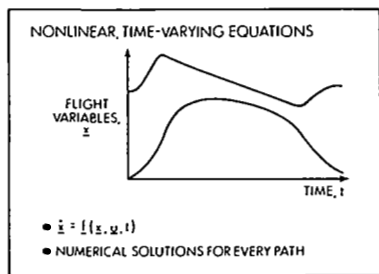
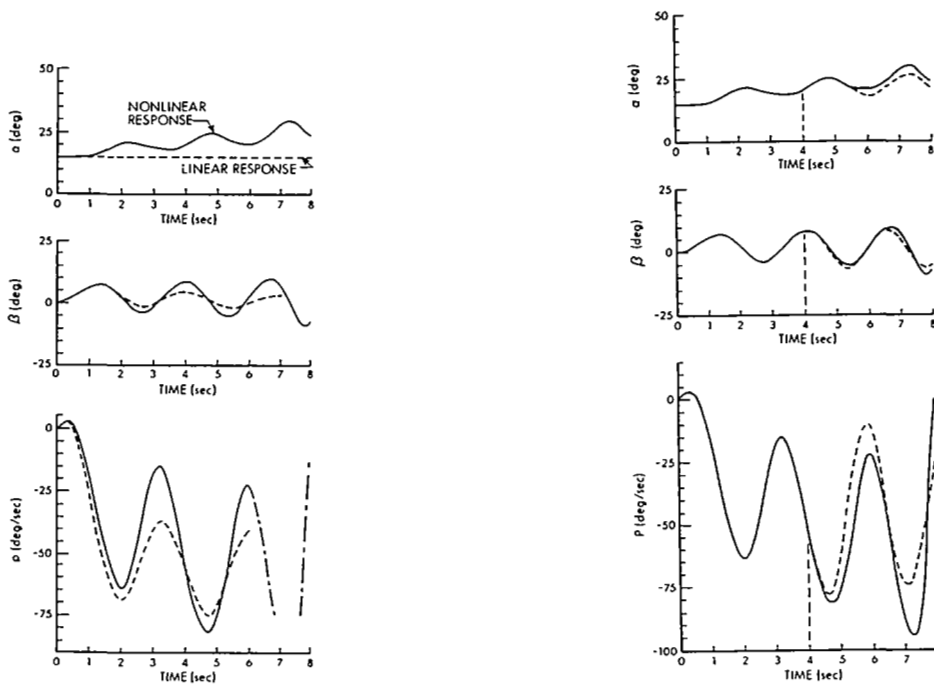
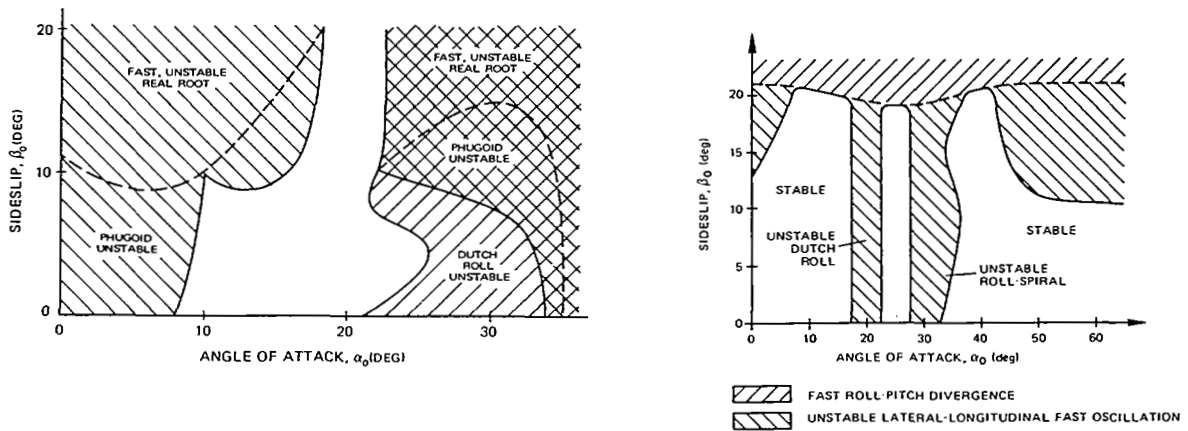


Figure 1.- Dynamic models for maneuvering flight.

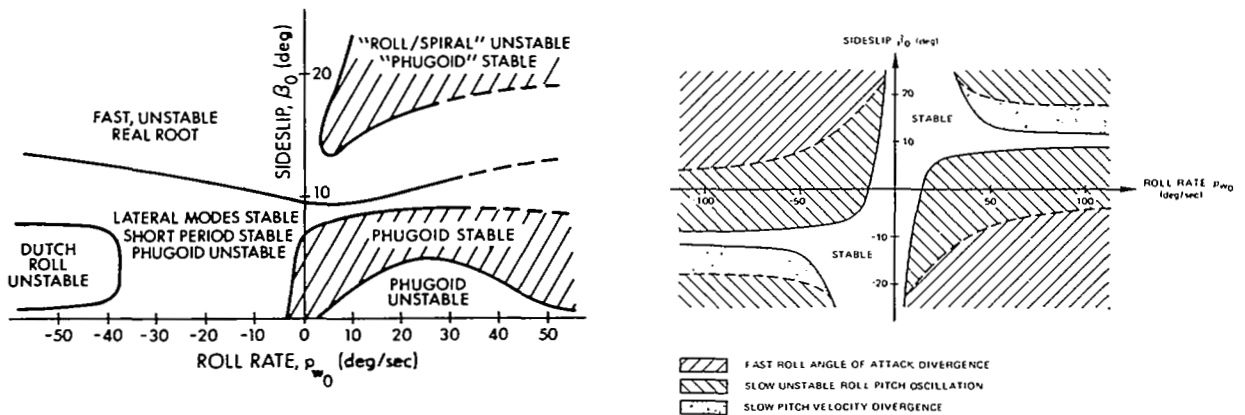


(a) Uncoupled linearization. (b) Coupled linearization.

Figure 2.- Comparison of responses of nonlinear and linear models to a large rudder input. (Aircraft A).



(a) Aircraft A: $V_0 = 94 \text{ m/s}$, (b) Aircraft B: $V_0 = 213 \text{ m/s}$.
 Figure 3.- Effects of mean angles of attack and sideslip on dynamic stability boundaries.



(a) Aircraft A: $V_0=94\text{m/s}$, $\alpha_0=15 \text{ deg}$. (b) Aircraft B: $V_0=213\text{m/s}$, $\alpha_0=10 \text{ deg}$.
 Figure 4.- Effects of combined sideslip angle and wind-axis roll rate on dynamic stability boundaries.

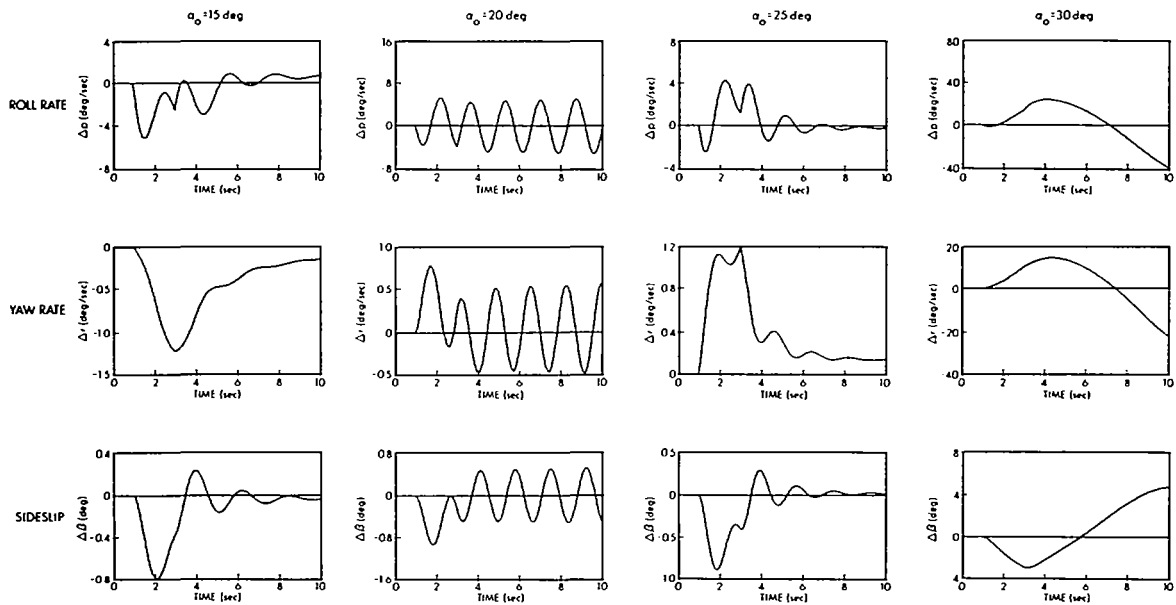
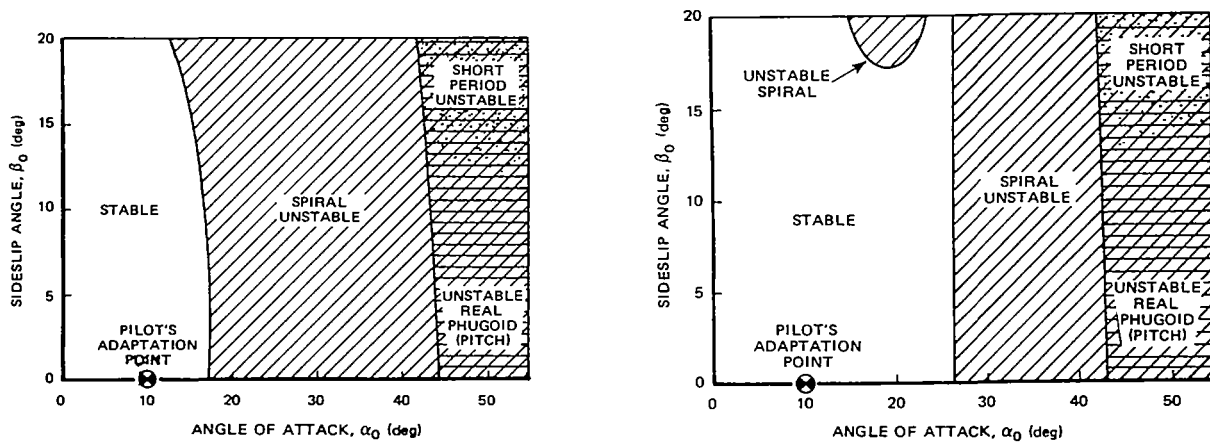


Figure 5.- Effects of increasing angle of attack on lateral control response. (Aircraft B).



(a) Pilot uses control stick only. (b) Pilot uses control stick and rudder pedals.

Figure 6.- Stability boundaries of aircraft B with pilot control. (Pilot uses control strategies appropriate to $\alpha_0 = 10$ deg.)

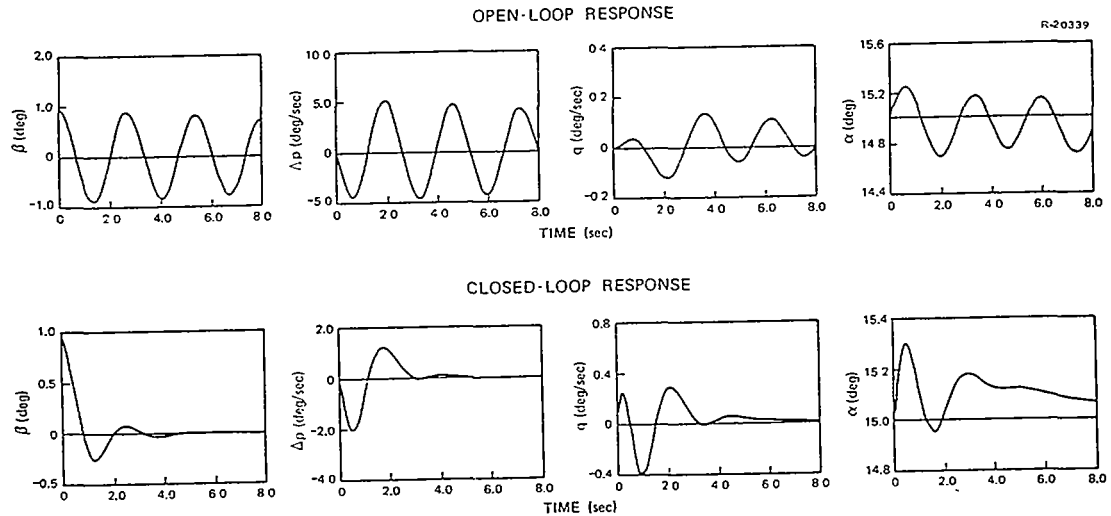


Figure 7.- Response of aircraft A to sideslip perturbation during constant-roll-rate maneuver. $p_{W_0} = 39.6$ deg/sec; $\alpha_0 = 15^\circ$; $V_0 = 94$ m/s.

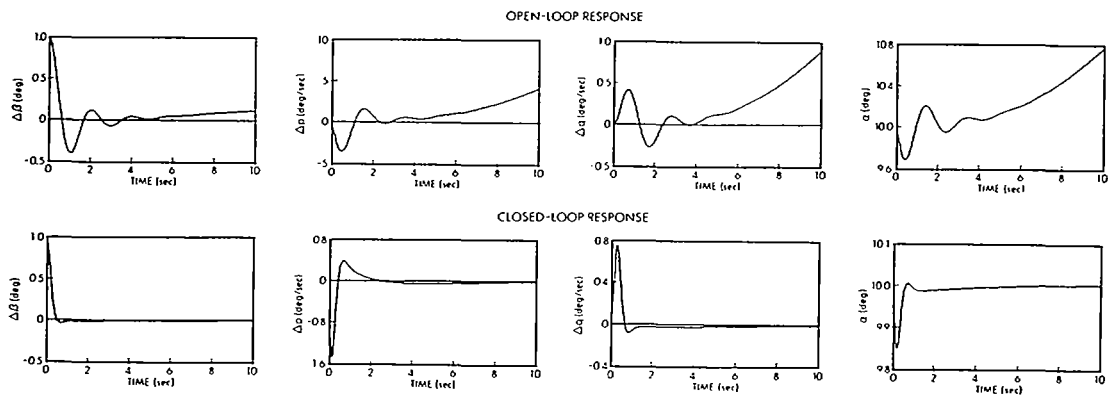


Figure 8.- Response of aircraft B to sideslip perturbation during constant-roll-rate maneuver. $p_{W_0} = 75$ deg/sec; $\alpha_0 = 10^\circ$; $V_0 = 213$ m/s.